Detection and Vertical Profiling of Airborne Pollen Using Fluorescence Lidar Measurements

G. Peletidou(a), K.A. Voudouri(b,a), K. Michailidis(a), S. Papadogiannaki(a), D.Balis(a)
(a) Aristotle University of Thessaloniki, Department of Physics, 54124 Thessaloniki, Greece
(b) National Observatory of Athens, Institute for Astronomy, Astrophysics, Space Applications and Remote Sensing, 15236 Athens, Greece
Lead Author e-mail address: gpeletid@auth.gr

Abstract: In this study, the upgraded Thessaloniki's lidar system is used to monitor the vertical distribution and optical characteristics of airborne pollen in the urban environment of Thessaloniki. Fluorescence backscattering coefficients and fluorescence capacity are retrieved and analyzed in combination with particle backscatter, particle linear depolarization ratio, and Ångström exponents to detect pollen aerosol layers. A case study from July 2025 revealed multiple aerosol layers, including a distinct layer characterized by enhanced fluorescence capacity (2.8×10^{-4}), indicative of pollen presence.

1. Introduction

Atmospheric aerosols play a vital role in Earth's climate, public health, and air quality. Traditional lidar systems, elastic, Raman, and high spectral resolution lidars, provide invaluable data on particle size, concentration, and optical properties, but they often lack the necessary retrievals to discriminate particle types such as biological species. Over the past decade, fluorescence lidar has emerged as a complementary technique capable of probing the biochemical composition and fluorescent characteristics of aerosols, greatly enhancing aerosol classification capabilities.

Fluorescence lidars offer the advantage of investigating the vertical distribution of pollen. Up to now extensive research has examined various aspects of airborne pollen in Thessaloniki, Greece [1-5]. These studies collectively emphasize not only the diversity of pollen taxa and their seasonal patterns, but also their allergenic relevance to the local population, the impact of meteorological conditions on their atmospheric behavior and the methodological approaches used to assess their presence and forecast concentrations. Thessaloniki hosts one of the most comprehensive and long-standing pollen monitoring stations in Southeastern Europe, operating continuously since 1987 [1,2]. The city's pollen spectrum, based on the airborne presence of 16 taxa, showed that Cupressaceae (24.9%), Quercus (20.8%), Parietaria (13.6%), Olea (9.1%), Pinaceae (8.9%) and Poaceae (6.3%) were dominant. Building on this foundation, Damialis et al. (2007) investigated long-term (1987-2005) pollen trends, revealing a general doubling in airborne concentrations per decade across many taxa. Significant increases were found for Cupressaceae, Quercus, Platanus and Pinaceae, attributed not to vegetation expansion but to environmental factors, especially temperature rise, underscoring the effects of climate change. Ziello et al. (2012) further showed that urban environments like Thessaloniki are particularly vulnerable to rising pollen levels, observing that urban pollen stations display stronger increasing trends than rural ones across Europe [3]. Paschalidou et al. (2020) classified synoptic circulation types and associated them with distinct seasonal pollen peaks, Carpinus, Cupressaceae and Quercus in winter, Olea and Urticaceae in spring-summer and Poaceae in late summer-autumn, demonstrating potential applications for early-warning systems [4]. Finally, Damialis et al. (2017) conducted one of the few vertical profiling studies in the region, using cars and aircraft to sample pollen at different elevations [5]. They confirmed the presence of high-altitude pollen, including Pinaceae and Quercus, up to 2000 m above ground. This suggested that once airborne, pollen grains can remain suspended and be transported farther than previously assumed, expanding the spatial domain of exposure.

Overall, fluorescence lidar measurements provide a valuable tool for advancing the investigation of the vertical distribution of pollen and for exploring additional pollen characteristics, such as size and shape. This study presents initial results of Thessaloniki's lidar system demonstrating this capability.

2. Instrument and Methods

Thessaloniki's lidar system (3β+2α+1δ+1wv+1G) include three β_{aer} wavelengths (355, 532, 1064 nm) and two α_{aer} wavelengths (355, 532 nm), alongside aerosol intensive properties such as backscatter and extinction-related Ångström exponents ($BAE_{355/532}$, $EAE_{355/532}$, $BAE_{532/1064}$), lidar ratio (LR_{532}, LR_{355}), linear volume ($VLDR_{532}$), particle depolarization ratio ($PLDR_{532}$), mixing ratio (MR_{408}) and fluorescence capacity (G_{466}). All signals undergo preprocessing and optical processing using the Single Calculus Chain (SCC) [7] algorithm, the fully automated algorithm, which has been developed to provide a common lidar processing tool, within European Aerosol Research Lidar Network (EARLINET: https://www.earlinet.org/) stations. However, SCC in its current version does not handle water vapor and fluorescence channels so for the new products the signals undergo preprocessing using the in-house semi-automated universal lidar algorithm (SULA) [8]. Additionally, quality assurance procedures for lidar signals are guaranteed using the Automated Lidar Analysis Software (ATLAS; https://github.com/nikolaos-siomos/ATLAS/releases/tag/v0.5.0) passing all the quality assurance standards established within EARLINET, to assure THELISYS high-quality products.

In this study, the fluorescence backscattering coefficient and fluorescence capacity were computed by adopting the method described by Veselovskii et al. 2020. This approach allows the retrieval of the aerosol backscattering coefficient from Mie–Raman lidar measurements without requiring a clear molecular reference height, due to the unknown fluorescence response of the background aerosol. The method is based on the ratio of the fluorescence signal to the nitrogen Raman signal and the aerosol backscattering coefficient $\beta_F(z)$ is then computed using the following relation:

$$\beta_F = \frac{C_R}{C_F}\frac{P_F}{P_R} N_R \sigma_R \frac{T_R}{T_F} \quad (1)$$

Once the fluorescence backscatter coefficient has been calculated, the fluorescence capacity G_F, can be quantified by evaluating its ratio to the total backscatter originating from aerosols at 532nm.

$$G_F = \frac{\beta_F}{\beta_{532}} \quad (2)$$

The backscattering and fluorescence capacity profiles presented in this work were derived using this methodology. Currently, our team has developed an in-house algorithm for calibrating the signals and calculating the optical properties of the new products.

3. Pollen case in Thessaloniki

Fluorescence measurements with the upgraded THELISYS have been taken since April 2024, providing a wide range of extensive and intensive properties to identify the detected aerosol layers. Here, we present a case study of a pollen episode observed on July 2, 2025. The properties of different aerosols are analyzed and for this the wavelet covariance transform (WCT) is used to identify multiple aerosol layers within a single profile and provides insight into internal layer structure when sufficient vertical variability is present in the backscatter signal [10,11].

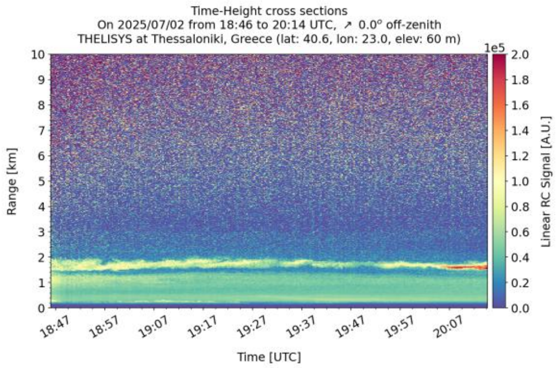

Figure 1. Temporal evolution of the fluorescence analog signal.

The retrieved vertical profiles of particle backscatter coefficients, fluorescence capacity and particle linear depolarization ratio are shown in Fig. 2a–c. Three distinct aerosol layers are identified with the wavelet covariance transformation. The first layer extends from 0.6 to 1.3 km, the second from 1.6 to 1.9 km, and the third from 2.9 to 3.1 km. The back-trajectory analysis demonstrates that the air masses on this day were transported from Balkans.

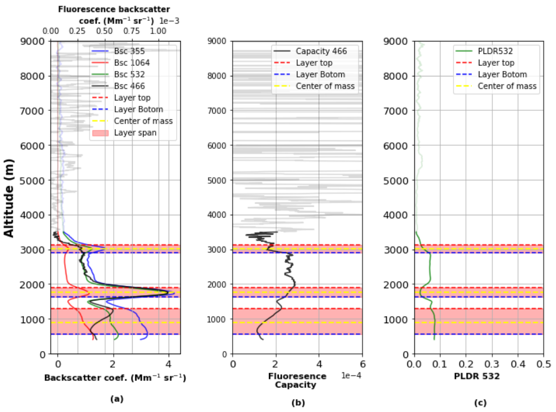

Figure 2. Vertical profiles of the backscatter coefficients (a), fluorescence capacity (b) and particle linear depolarization ratio (c) on 02/07/2025.

Mean values of the optical properties were calculated for each layer. In the first layer, the mean fluorescence capacity is 1.6×10^{-4}, the PLDR is 0.07, and the $BAE_{355/532}$ is 1.06, indicating the presence of urban aerosols.

The second layer exhibits a higher mean fluorescence capacity (2.8×10^{-4}), a lower PLDR (0.02), and a lower $BAE_{355/532}$ (0.22). These values, particularly the high fluorescence capacity at this altitude, together with the absence of confirmed biomass-burning aerosols on that day, suggest the presence of pollen. Veselovskii et al. (2021) reported that fluorescence capacity values are high around 1.5×10^{-4} and PLDR values at 532 nm around 0.15 for pollen in Lille, while Filioglou et al. (2023) found higher PLDR values, with approximately 0.28 for birch pollen and 0.43 for pine pollen in Kuopio. The observed linear particle depolarization ratios for the mixed pollen layer, representing the first such measurements in Mediterranean countries, differ from those reported at more northern latitudes, reflecting differences in pollen type. In Thessaloniki, during July, Urticaceae pollen is present in the atmosphere (Fig. 3), and these pollen grains are considered as spherical from the existing literature [14, 15].

Finally, the third layer shows mean values similar to those of the first layer, with a fluorescence capacity of 1.8×10^{-4}, a PLDR of 0.04, and a $BAE_{355/532}$ of 0.76, again indicating urban aerosols.

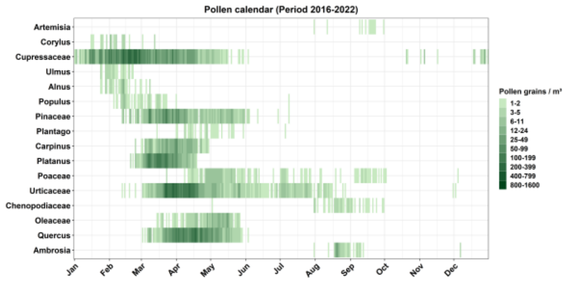

Figure 3. Pollen seasonal concentration for 2016-2022.

4. Conclusions

This study demonstrates the potential of fluorescence lidar measurements for the detection and vertical characterization of pollen over Thessaloniki. By exploiting fluorescence capacity in combination with other aerosol optical properties, distinct aerosol layers could be differentiated, and mixed pollen layers can be identified at different elevated altitudes. The analyzed case study showed that higher fluorescence capacity values ($G_{466} > 2 \times 10^{-4}$) at altitudes up to 2.5 km can be attributed to the presence of pollen. These results demonstrate that fluorescence lidar observations can be used to identify pollen layers and distinguish them from other aerosol types. Moreover, we highlight the added value of fluorescence channels for aerosol typing, which provide a promising framework for future continuous monitoring of pollen transport and exposure, with important implications for air quality assessment and public health.

5. Acknowledgments

Part of this work was supported by the COST Action EARLICOST (CA24135), supported by COST (European Cooperation in Science and Technology).

6. References

[1] A. Damialis et. al., "Long-Term Trends in Atmospheric Pollen Levels in the City of Thessaloniki, Greece." *Atmos. Environ. 41*, 7011–7021 (2007).

[2] Papadogiannaki, S., Karatzas, K., Kontos, S., Poupkou, A., Melas, D.: A Multi-Model Approach to Pollen Season Estimations: Case Study for Olea

and Quercus in Thessaloniki, Greece. Atmosphere, 16, 454 (2025).

[3] D. Gioulekas et. al., "Allergenic Pollen Records (15 Years) and Sensitization in Patients with Respiratory Allergy in Thessaloniki, Greece." Allergy 59, 174–184 (2004).

[4] C. Ziello et al., "Changes to Airborne Pollen Counts across Europe." PLoS One 7 (2012).

[5] A.K. Paschalidou et. al., "Identifying Patterns of Airborne Pollen Distribution Using a Synoptic Climatology Approach." Sci. Total Environ. 714, 136625 (2020).

[6] A. Damialis et. al.: Estimating the Abundance of Airborne Pollen and Fungal Spores at Variable Elevations Using an Aircraft: How High Can They Fly? , Sci. Rep. 7, 1–11 (2017).

[7] G. D'Amico et. al.: EARLINET Single Calculus Chain – overview on methodology and strategy., Atmos. Meas. Tech. 8, 4891–4916 (2015).

[8] Paschou, P. et al.: The eVe reference polarisation lidar system for the calibration and validation of the Aeolus L2A product, Atmos. Meas. Tech., 15, 2299–2323 (2022).

[9] I. Veselovskii et. al.: Combined use of Mie–Raman and fluorescence lidar observations for improving aerosol characterization: feasibility experiment., Atmos. Meas. Tech. 13, 6691–6701 (2020).

[10] Baars, H., Ansmann, A., Engelmann, R., and Althausen, D.: Continuous monitoring of the boundary-layer top with lidar, Atmos. Chem. Phys., 8, 7281–7296 (2008).

[11] N. Siomos, et. al.: Are EARLINET and AERONET climatologies consistent? The case of Thessaloniki, Greece." Atmos. Chem. Phys. 18, 11885–11903 (2018).

[12] Veselovskii, I., et al.: Mie–Raman–fluorescence lidar observations of aerosols during pollen season in the north of France, Atmos. Meas. Tech., 14, 4773–4786 (2021).

[13] Filioglou, M., et. al.: Spectral dependence of birch and pine pollen optical properties using a synergy of lidar instruments, Atmos. Chem. Phys., 23, 9009–9021 (2023).

[14] Komnos I., et. al.: A Study of Airborne Pollen Grains and Fungal Spores in the Region of Epirus (Northwestern Greece). Cureus 14(6): e26335. doi:10.7759/cureus.26335 (2022).

[15] Smith, E. G.: Sampling and identifying allergenic pollens and molds: An illustrated identification manual for air samplers. Blewstone Press (1984).